Hydrol. Earth Syst. Sci. Discuss., 12, 7785–7819, 2015
www.hydrol-earth-syst-sci-discuss.net/12/7785/2015/
doi:10.5194/hessd-12-7785-2015
© Author(s) 2015. CC Attribution 3.0 License.

Hydrology and Earth System Sciences
Open Access
Discussions

This discussion paper is/has been under review for the journal Hydrology and Earth System Sciences (HESS). Please refer to the corresponding final paper in HESS if available.

Impacts of land use change and climate variations on annual inflow into Miyun Reservoir, Beijing, China

J. K. Zheng[1,3], G. Sun[2], W. H. Li[3], X. X. Yu[4], C. Zhang[3], Y. B. Gong[1], and L. H. Tu[1]

[1]College of Forestry, Sichuan Agricultural University, Chengdu, Sichuan 611130, China
[2]Eastern Forest Environmental Threat Assessment Center, USDA Forest Service, 920 Main Campus, Venture II, Suite 300, Raleigh, NC 27606, USA
[3]Earth and Ocean Sciences, Nicholas School of the Environment, Duke University, Durham, NC 27708, USA
[4]School of Soil and Water Conservation, Beijing Forestry University, Beijing 100083, China

Received: 27 June 2015 – Accepted: 29 June 2015 – Published: 11 August 2015

Correspondence to: J. K. Zheng (jiangkunzheng@126.com)

Published by Copernicus Publications on behalf of the European Geosciences Union.

Abstract

Miyun reservoir, the only surface water source for Beijing city, has experienced water supply decline in recent decades. Previous studies suggest that both land use change and climate contributes the changes of water supply in this critical watershed. However, the specific causes of the decline in Miyun reservoir are debatable in a non-stationary climate in the past four decades. The central objective of this study was to quantify the separate and collective contributions of land use change and climate variability to the decreasing inflow into Miyun reservoir during 1961–2008. Different from previous studies, this work objectively identified breakpoints by analyzing the long-term historical hydrometeorology and land cover records. To effectively study the different impacts of the climate variation and land cover change during different sub-periods, annual water balance model (AWB), climate elasticity model (CEM), and rainfall–runoff model (RRM) were employed to conduct attribution analysis synthetically. We found a significant decrease in annual streamflow ($p < 0.01$), a significant positive trend in annual potential evapotranspiration ($p < 0.01$), and an insignificant negative trend in annual precipitation ($p > 0.1$) during 1961–2008. Combined with historical records, we identified two breakpoints as in 1983 and 1999 for the period 1961–2008 by the sequential Mann–Kendall Test and Double Mass Curve. Climate variability alone did not explain the decrease in inflow to Miyun reservoir. Reduction of water yield was closely related to increase in evapotranspiration rates due to the expansion of forestlands and reduction in cropland and grassland, and was likely exacerbated by increased water consumption for domestic and industrial uses in the basin. Our study found that the contribution to the observed streamflow decline from land use change fell from 64–92 % during 1984–1999 to 36–58 % during 2000–2008, whereas the contribution from climate variation climbed from 8–36 % during the 1984–1999 to 42–64 % during 2000–2008. Model uncertainty analysis further demonstrated that climate warming played a dominant role in streamflow reduction in the 2000s. We conclude that future climate change and variability will further challenge the goal of water supply of Miyun reservoir to meet

HESSD
12, 7785–7819, 2015

water demand. A comprehensive watershed management strategy needs to consider the climate variations besides vegetation management.

1 Introduction

Land use change and climate variations are two main factors directly affecting the watershed hydrological cycle. Land use change influences watershed water yield by changing canopy interception, soil properties, biophysical factors affecting evapotranspiration, and groundwater use whilst climate variations alters precipitation, air temperature, humidity, plant growth, and consequently the hydrologic balances (Baker and Miller, 2013; Wang et al., 2013). Meanwhile, interactions of land use change and climate variations are complex and understanding the individual effects on watershed water yield is of great importance for land-use planning and water resource management (Zheng et al., 2013). To optimize watershed management and allocate limited resources, it is important to assess hydrological impacts of climate variations and land use change separately and collectively (Mango et al., 2011). A clear understanding of the driving factors for watershed hydrology also benefits hydrological model development and evaluation methods (Wang et al., 2013). Due to the nonlinearity of streamflow response in the synchronous evolution of driving forces, it is challenging to disentangle the integrative effects of climate forcing and basin characteristics (Risbey and Entekhabi, 1996; Beguería et al., 2003; Arabi et al., 2007; Morán-Tejeda et al., 2010). Many methods have been developed for isolating the effect of land use change from climate variations on regional hydrology. These methods include paired catchment approach (Brown et al., 2005; Zégre et al., 2010), statistical methods (Costa et al., 2003; Sun et al., 2006; Petchprayoon et al., 2010), and hydrological model (Haverkamp et al., 2005; Mao and Cherkauer, 2009; Baker and Miller, 2013). Raymond et al. (2008) suggested that land use change and management were more important than climate variation to increase riverine water export from Mississippi River over the past 50 years. However, other studies considered climate

HESSD
12, 7785–7819, 2015

change as a dominant cause of annual water yield change (Aguado et al., 1992; Christensen et al., 2004; Barnett et al., 2005; Sun et al., 2013). Thus detecting the hydrologic changes in observed streamflow records must consider both land use change and climatic variation.

Miyun reservoir provides 70 % of total water supply for Beijing and is the only source of surface water supply for the severe water stressed megacity with a population of 20 million (Tang et al., 2011). Over the past half-century, streamflow into the Miyun reservoir had shrunk drastically. Mean inflow into the Miyun Reservoir declined from 88.2 $m^3 s^{-1}$ in the 1950s to 15.8 $m^3 s^{-1}$ in the 1980s (Gao et al., 2002). Meanwhile, population in Beijing increased from 2.8 million in 1953 to 20 million today (Liu et al., 2003). The contradiction between increasing water demand and water shortage constrains economic and social development of the region. Therefore, water resource assessment is extremely important to develop effective management strategies.

A few studies have tried to isolate hydrological impacts of land use change from climate change on streamflow in Miyun reservoir catchment (MYRC) (Wang et al., 2009, 2013; Xu et al., 2009; Ma et al., 2010; Zhan et al., 2011; Bao et al., 2012a). However, conclusions varied significantly. For example, Wang et al. (2009) and Ma et al. (2010) considered that climate impact separately accounted for about 33 and 55 % of the decrease in reservoir inflow using the distributed time-variant gain model and geomorphology-based hydrological model. The discrepancies are mainly caused by assessment methodology due to parameter uncertainty (Shen et al., 2012), diversities of structural complexity (Velázquez et al., 2013), inconsistent of evaluation period (López-Moreno et al., 2011). It is impracticable to get an exact hydrological effect of land use and climate change. Hence, Wei et al. (2013) recommended that a combination of two or three methods would be a robust research strategy to assess hydrological effect within a certain range. In this research, the relative contributions of land use change and climate variability to changes of the annual streamflow into Miyun reservoir were quantified using annual water balance model based on Zhang et al. (2001), the climate elasticity model (Sankarasubramanian et al., 2001),

HESSD
12, 7785–7819, 2015

and rainfall–runoff models (Jones et al., 2006) for understanding water cycles and balance in the study area. To our knowledge, the present work is the first study to comprehensively examine the hydrologic effects of vegetation change under a non-stationary climate using a long-term hydrological and land use record.

Our objectives are to: (1) detect the trend and break points of streamflow series for the period from 1961 to 2008, (2) explore an integrated approach to evaluate phased effects of climate and land use change on the inflow into Miyun reservoir, and (3) provide suggestion to watershed management for the studied watershed.

2 Materials and methods

2.1 Catchment characteristic

Miyun reservoir, located about 100 km to the north of downtown Beijing, was built in 1960. The reservoir that received water from the Chao River and the Bai River, has a total storage capacity of approximately 4.4 billion m^3, enough to supply more than half of water supply for Beijing City (Dong and Li, 2006). The drainage area is about 15 380 km^2 (115°25′, 117°33′ E, 40°19′, 41°31′ N), occupying nearly 90 % of the Chaobai River basin area (Fig. 1). The local climate is characterized as temperate monsoon and semi-arid (Xu et al., 2009). MYRC drains nine counties of Hebei Province and three counties of Beijing City. The total landmass of Chicheng, Guyuan, Luanping, and Fengning counties in Heibei Province accounts for 77 % of the whole catchment area (Wang, 2010). The population of the four counties increased from 0.95 million during 1961–1983 to 1.18 million during 1984–1999, and further to 1.23 million during 2000–2008 (Fig. 2). Land use maps were converted from the 1 : 100 000 land-use map of China, which was obtained from the Resources and Environment Data Center of CAS (http://www.resdc.cn/data_Resource/dataResource.asp). Based on data availability and model building, land use maps of sub catchments were used including Yuzhoushuiku (YZSK), Xiabao (XB), Sandaoying (SDY), Zhangjiafen (ZJF),

HESSD
12, 7785–7819, 2015

Dage (DG), Daiying (DY), Xiahui (XH) in 1978, 1988, 1998, and 2008; Huaihe (HH), Hongmenchuan (HMC), Banchengzi (BCZ) in 1990, 1995, 2000, and 2005; Tumen (TM) in 2000, and 2005 (Fig. 1). Land use was regrouped into six categories, i.e., water area, bare area, forestland, cropland, grassland, and residential area.

2.2 Hydro-meteorological data

Daily precipitation data recorded at 37 rainfall gauges and daily discharge data of 11 hydrological stations were obtained from "Hydrological Year Book" by the China Hydrological Bureau. Daily meteorological data for the period of 1961–2008, including precipitation, air temperature (maximum, minimum, and mean), wind speed, relative humidity, and sunshine hours of 7 meteorological stations (Zhangbei, Fengning, Weichang, Zhangjiakou, Huailai, Chengde, and Beijing) were obtained from the China Administration of Meteorology.

Average monthly temperatures from November to February were below 0 °C Minimum monthly temperature in January was lowest at −15 °C and maximum monthly temperature in July was highest at 29 °C. Precipitation (P) in summer (June, July, and August) accounted for 68 % of annual total precipitation. In comparison, potential evapotranspiration (E_p) in summer, accounted for 48 % of annual totals. It indicated a more uneven seasonal distribution of P than that of E_p (Fig. 3).

2.3 Detecting the break points of streamflow time series

Both the Double Mass Curve (Searcy and Hardison, 1960) and the sequential version of Mann–Kendall test (Mann, 1945; Sneyers, 1975) were applied to detect the break points. The Double Mass Curve is the curve through the points given two cumulative records. A break in this curve indicates a change in the relationship between the two records that may be caused by the processing of the data (Wigbout, 1973). A non-parametric test method, the sequential version of Mann–Kendall test is used to detect

HESSD
12, 7785–7819, 2015

the change point of hydrological data series:

$$S_k = \sum_{i=1}^{k} r_i \ (k = 2, 3, \ldots, n) \tag{1}$$

Where r_i is as following:

$$r_i = \begin{cases} +1(x_i > x_j) \\ 0(x_i \leq x_j) \end{cases} (j = 1, 2, \ldots, i) \tag{2}$$

For each comparison, the number of cases $x_i > x_j$ is counted, and denoted by r_i. It is assumed that the statistic sequential values are random and independent. Then statistic variance (UF_k) is defined as follows:

$$\mathrm{UF}_k = \frac{[s_k - E(s_k)]}{\sqrt{\mathrm{Var}(s_k)}} \ (k = 1, 2, \ldots, n) \tag{3}$$

$$E(s_k) = \frac{n(n+1)}{4} \tag{4}$$

$$\mathrm{Var}(s_k) = \frac{n(n+1)(2n+5)}{72} \tag{5}$$

where $E(s_k)$ and $\mathrm{Var}(s_k)$ are mean and variance of s_k, respectively. Statistic variance UF_k is calculated as the forward data series ($\mathrm{UF}_1 = 0$). The backward sequence UB_k is calculated using the same equation but in the reverse data series. A null hypothesis is accepted if the critical value ($u_{0.05}$) lies within ±1.96 at a significance level ($\alpha = 0.05$). The positive UF_k denotes an upward trend while the reverse series as a downward trend. When the value of UF_k exceeds the critical value ($u_{0.05}$), it demonstrates an upward or downward trend significantly. If there are intersections of UF_k and UB_k lines in the range of critical value ($u_{0.05}$) the first cross point is the break point.

HESSD
12, 7785–7819, 2015

2.4 Hydrological models for attribution analysis

In this paper, climate variations primarily refer to the changes of P and E_p. Due to difficulty in quantitatively describing anthropogenic effects including water withdrawal and water consumption, land use change is acted as the residuals affecting streamflow (Q) in addition to climate variations following Stohlgren et al. (1998) and Ma et al. (2010). Three models were built to provide a comprehensive evaluation on streamflow decreases in MYRC.

2.4.1 Annual water balance model (AWB)

To detect the influence of land use change on Q, a model was developed based on the sensitivity of land use change to actual evapotranspiration (E_a) (Zhang et al., 2001). Formulates were described as follows.

$$Q = P - E_a \pm \Delta\delta \tag{6}$$

$$E_a = \frac{1 + \omega\frac{E_p}{P}}{1 + \omega\frac{E_p}{P} + \frac{P}{E_p}} \cdot P \tag{7}$$

$$E_{a(tot)} = \sum_{i=1}^{n} (E_{a(i)} \cdot f_i) \tag{8}$$

$$E_p = 0.1651 D V_d K (E_p = 0 \text{ when } T < 0) \tag{9}$$

$$V_d = 216.7 V_s / (T + 273.3) \tag{10}$$

$$V_s = 6.108 \cdot \exp(17.26939 T / (T + 273.3)) \tag{11}$$

where δ (mm) is the water storage change of the watershed which can be neglected at long-time averages (Donohue et al., 2010). At a meso-scale, the watershed annual Q (mm yr^{-1}) can be estimated as the difference between the P (mm yr^{-1}) input and the E_a (mm yr^{-1}) output (Sun et al., 2005). ω is the plant-available water coefficient

HESSD
12, 7785–7819, 2015

that varies in soil water use for transpiration. For MYRC, ω values of different land use, as a key indicator, were estimated by trial and error approach with increments in 0.1 using a computer program. f_i is the percentage of land use area, in which i represents diverse landscapes: forestland, grassland, cropland, water area, residential area, and bare area. $E_{a(tot)}$ is the sum of $E_{a(i)}$. E_p (mm day^{-1}) was calculated using Hamon method (Hamon, 1963; Lu et al., 2005). D is the day length (h). V_d is saturated vapor density at the daily average temperature (g m^{-3}), K is the correction factor. T is the daily average temperature (°). V_s is the saturated vapor under a certain temperature (mbar).

2.4.2 The climate elasticity model (CEM)

To quantitatively evaluate the influence of climate variation on streamflow, the climate elasticity model (CEM) was built. The CEM defines the proportional change of streamflow divided by the proportional change in a climate variable such as precipitation (Ma et al., 2010). The model was first developed by Schaake and Waggoner (1990) to evaluate the sensitivity of streamflow to climate changes, and then employed widely to assess the climate variability impact (Sankarasubramanian et al., 2001; Jones et al., 2006; Fu et al., 2007; Bao et al., 2012b).

$$\frac{\Delta Q_i}{\overline{Q_0}} = \varepsilon_1 \frac{\Delta P_i}{\overline{P}} + \varepsilon_2 \frac{\Delta E_{p(i)}}{\overline{E_p}} \tag{12}$$

$$d\overline{Q}_{clim} = \overline{Q_e} - \overline{Q_0} \tag{13}$$

$$d\overline{Q}_{land} = \overline{O_e} - \overline{Q_e} \tag{14}$$

$$d\overline{Q}_{tot} = d\overline{Q}_{clim} + d\overline{Q}_{land} \tag{15}$$

Where ε_1 and ε_2 are elasticity coefficients for P (mm yr^{-1}) and E_p (mm yr^{-1}), respectively, which are estimated by least square estimation with the Matlab7.0. $\overline{Q_0}$

HESSD
12, 7785–7819, 2015

($\mathrm{mm\,yr^{-1}}$), $\overline{P}$ ($\mathrm{mm\,yr^{-1}}$) and $\overline{E_p}$ ($\mathrm{mm\,yr^{-1}}$) refer to the mean annual Q, P and E_p in the reference period. ΔP_i and $\Delta E_{p(i)}$ are the change of annual P and E_p compared to $\overline{P}$ and $\overline{E_p}$, respectively. Annual Q ($\mathrm{mm\,yr^{-1}}$) for the periods 1984–1999 and 2000–2008 can be derived from Eq. (12) and calculated into mean value ($\overline{Q_e}$). $\mathrm{d}\overline{Q}_{\mathrm{clim}}$ is the average change in Q caused by climate impact. $\mathrm{d}\overline{Q}_{\mathrm{land}}$ is the average change in Q cause by land use change, and $\mathrm{d}\overline{Q}_{\mathrm{tot}}$ is the average change in Q between the reference period and evaluation period. $\overline{O_e}$ and $\overline{Q_e}$ are the average annual Q observed and simulated during the evaluation periods, respectively.

2.4.3 Rainfall–runoff model (RRM)

In addition to the CEM method discussed in Sect. 2.4.2, the impact of climate variability on streamflow was also estimated using the following empirical rainfall–runoff models (Jones et al., 2006; Li et al., 2007).

$$Q_i = a + bP_i(\sigma_i^2)^c \tag{16}$$

$$\mathrm{d}\overline{Q}_{\mathrm{clim}} = \overline{Q_e} - \overline{Q_r} \tag{17}$$

Here, Q_i ($\mathrm{mm\,yr^{-1}}$) and P_i ($\mathrm{mm\,yr^{-1}}$) are the annual observed streamflow and precipitation, respectively. σ_i^2 is the variance of the monthly precipitation; a, b, and c are constants determined by hydrometeological data in the reference period. $\overline{Q_e}$ ($\mathrm{mm\,yr^{-1}}$) and $\overline{Q_r}$ ($\mathrm{mm\,yr^{-1}}$) are the average simulate annual streamflow during the evaluation period and reference period, respectively.

HESSD
12, 7785–7819, 2015

3 Results

3.1 Land use change and its major driving factors

In the Miyun Reservoir catchment, forestlands accounted for above half of the total area. Compared to 1978, forestland area increased by 5.0 % in 1988, 16.3 % in 1998 and 18.2 % in 2008, respectively, whereas cropland decreased by 6.6, 8.7, and 10.8 % correspondingly. Meanwhile, grassland enlarged from 16.5 % in 1978 to 18.5 % in 1988, and then reduced to 10.4 % in 1998, and 9.8 % in 2008 (Fig. 4). National land policies are the main driving forces to the land cover change. Since January 1982, implementation of the household contract responsibility system has brought a huge impact on cropland and forestland. Reforestation has been widely implemented to develop forest industry and tourism especially along with implementation of "Grain for Green" and "Beijing-Tianjin sandstorm source control project" since later 1990s (Zheng et al., 2010).

3.2 Evolution and break points of annual streamflow series

As described in Fig. 5, a significant decreasing trend at the rate of 0.96 mm yr^{-1} was observed for annual streamflow during 1961–2008 ($p < 0.01$). Simultaneously, PET increased by 1.25 mm yr^{-1} significantly ($p < 0.01$) and precipitation decreased by 0.45 mm yr^{-1} insignificantly ($p > 0.1$) (Fig. 3). In Chao River basin and Bai River basin, break points occurred in different years according to different methods. Using the Ordered Clustering analysis method, one break point at 1979 was detected in the runoff record in the river basins (Wang et al., 2009). Yang and Tian (2009) found that abrupt changes in runoff occurred in 1983 and 1980 for Chao River basin and Bai River basin, respectively, based on the sequential Mann–Kendall test. Owing to significantly increasing direct water abstraction from the upstream of the reservoir since 1984, two sub-periods, one from 1956 to 1983 and the other from 1984 to 2005, were detected for Chao and Bai River basins (Ma et al., 2010). Tang et al. (2011) noted that

HESSD
12, 7785–7819, 2015

soil conservation practice positively affected the intensification reduction of streamflow after 1999. In this study, the sequential Mann–Kendall test was used to graphically illustrate the forward and backward trends of streamflow for Miyun Reservoir basin during 1961–2008. Intersection point of the UF_k and UB_k curves inside the dotted lines indicated that the year of 1984 was the starting point of such an abrupt change. In addition, changes in streamflow from 2000 to 2008 were more significant because points of the curves fall outside the dotted lines (Fig. 6). Furthermore, the Double Mass Curve was also used to divide annual streamflow series into three phases as in Fig. 7. Combined sequential Mann–Kendall test analysis with the double-mass curve test, we determined the referenced period (1961–1983), the evaluation period I (1984–1999), and the evaluation period II (2000–2008) in MYRC.

3.3 AWB model results

A total of 41 catchments with different land use composition were used to build the model. According to plant-available water coefficient w of different land use in AWB model, the watersheds were composed of forestland, grassland/cropland, water area and residential/bare area. Forestland accounts for more than 50 % of the whole area in DG, DY, XH, YZSK, SDY, XB, and ZJF watershed; more than 80 % of the total landmass in BCZ, HMC, and HH watershed; 100 % of total area in TM watershed (Fig. 8). The model was calibrated with the data prior to 2001 and was validated with the data after 2001 (Fig. 9). The range of w values was determined to be [0, 3] for forestland, [0, 2] for grassland/cropland, and [0, 1] for residential area/bare area. The E_a of water area was assumed to be the smaller between P and E_p. Based on the method of trial and error, w values of grassland/farmland, forest, urban/bare land were ratified as 1.5, 2.8, and 0 during the calibrated period, respectively. Compared the average annual water balance residual $E_a = P - Q$ with that estimated using Eqs. (7) and (8), the determination coefficients were 0.803 and 0.783 during calibration period and validation period, respectively (Fig. 9).

HESSD
12, 7785–7819, 2015

Compared to the reference period (1961–1983), annual observed streamflow for 1984–1999 and 2000–2008 reduced by 18.1 and 39.7 mm, respectively. Using the land use data in 1988, the model was applied to evaluation periods. The difference of observed value and simulated value represented the impacts of land use change on inflow declines. As showed in Table 1, $d\overline{Q}_{land}$ were −11.5 and −19.6 mm which contributed 64 and 49 % of $d\overline{Q}_{tot}$ for evaluation period I and II, respectively.

3.4 CEM model results

Annual Q, P, and E_p during the period of 1961–1983 were used to determine the parameter ε_1 (2.12) and ε_2 (−2.25) in Eq. (12). Then the model was applied to simulate the annual Q during the period of 1961–2008. The difference of Q between the simulation period of 1984–2008 and the reference period of 1961–1983 was attributed to the impact of climate variation. Simulated annual Q values were 57.7 and 42.6 mm during the periods of 1984–1999 and 2000–2008, respectively. The contribution of climate variation to the decrease of inflow during these two periods is about 1.5 mm (8 %) and 16.5 mm (42 %), respectively. Correspondingly, land use change contributed 16.6 mm (92 %) and 23.2 mm (58 %) to the decrease of inflow (Table 1).

3.5 RRM model results

Using annual P and the variance of the monthly P from 1961 to 1983, the values of a, b, and c were obtained as 0.85, 0.0004, and 0.74 from Eq. (14), respectively. Then annual inflow into the reservoir was simulated as 56.4 and 33.8 mm for evaluation period I and II, respectively. Derived from Eq. (15), climate variation constituted for 2.7 mm (15 %) and 25.3 mm (64 %) of total Q decrease for these two periods (Table 1). Compared to estimations from the CEM model, the contribution of climate variations to the decrease of inflow was about 7 % higher during the period of 1984–1999, and 22 % lower during the period of 2000–2008.

HESSD
12, 7785–7819, 2015

4 Discussion

4.1 Data limitation and impact of other human factors on streamflow

This study involved multiple years and multiple data sources for land use, meteorology, and hydrology. The bias of data often existed in field measurements, inventory, aggregation and spatial analysis of long series spatiotemporal data (Kavetski et al., 2006; Verburg et al., 2011). In the process of building the annual water balance model, 30 land use scenarios were utilized to calibrate the model and 11 land use scenarios were employed to verify it. To some extent, land use images were not absolutely comparable because the data were interpreted from different day of a year. Meanwhile, artificial interpretation of remote sensing imageries also increases possibility of the errors. Due to data limitation, only 37 rainfall gauges and 7 meteorological stations were available to clarify spatial change of precipitation, air temperature, and other meteorological elements, which might be insufficient to cover a mountainous catchment area of 15 380 km^2. Certainly, interpolation and calculation of spatial data also constitute integral parts of the error.

Since the 1980s, water uses in MYRC have been intensified due to the increased water demand by people (Bao et al., 2012a). On the one hand, due to the growth of population (Fig. 2) and development of industry and agriculture, the annual direct abstraction of water from MYRC increased from 2.2 $mm\,yr^{-1}$ in 1956–1983 to 13.4 $mm\,yr^{-1}$ in 1984–2005 (Ma et al., 2010). At the same time, daily water consumption per capita accrued from 0.03 m^3 in 1959 to more than 0.20 m^3 in 2000 (Gao et al., 2002). Population growth aggravates water scarcity because it reduces per-capita availability even with unchanged water resources (Schewe et al., 2014). Meanwhile, soil and water conservation projects have been implemented considerably with slopes transformed into terraces, the construction of silt retention dams and reservoirs in 1970s and 1980s (Chaobai River Management Bureau of Beijing, 2004; Chang et al., 2015). For example, The Yunzhou Reservoir (113.7 million m^3) and Baihebao Reservoir (90.6 million m^3) were built in 1970 and 1983, respectively. In

HESSD
12, 7785–7819, 2015

addition to water consumption, these water control projects enhanced evaporation and leakage losses from the catchment (Gao et al., 2013). Consequently, total water loss from the catchment had increased since the 1980s. In recent years, Paddy to Dry Land Project and closedown of water-based industries were carried out to reduce water consumption that might compensate the streamflow decline trend and improve water quality (Wang, 2010).

4.2 Model uncertainties

Three different approaches were used to isolate hydrological impacts of land use change from those of climate change. AWB offered direct approach to evaluate hydrological impacts of land use change (Zhang and Wang, 2007). E_p, as the predominant part of water cycle, is the key to build this model. It is attributed primarily to land cover, and also affected by several other factors such as soil types and topographic slope (Moiwo et al., 2010). The daily E_a (mm day^{-1}) might be estimated by the Surface Energy Balance Algorithm for Land (SEBAL), remote sensing-based models validated by the Penman–Monteith approach, as well as the Soil and Water Assessment Tools (SWAT) model (Gao and Long, 2008; Gao et al., 2008). Mean annual evapotranspiration to P, E_p, ω had been derived from numerous catchments (Zhang et al., 2001). Then a simple two-parameter model based on these coefficients was applied to many other catchments (Sun et al., 2005; Ma et al., 2008; Zhang et al., 2008). The Penman–Monteith method is commonly considered as the best way to estimate the value of E_p. However, the application was difficult due to insufficient climate data, especially variable about solar radiation. Therefore, the Hamon method recommended by the Food and Agriculture Organization of United Nations (FAO) was used to calculate E_p (Hamon, 1963). Our research specified an analytical expression to determine the value of model parameter (ω) as 2.8 and 1.5, respectively, for forestland and grassland/cropland, whose correlation coefficients are 0.78 and 0.80 during calibration and validation phases, respectively. The error of data, combined with uncertainty of model structure, increased uncertain to attribution of land use change.

HESSD
12, 7785–7819, 2015

Meanwhile, to detect the potential streamflow response of land use change in MYRC, the model adopted the land use data in 1988 to estimate streamflow since 1984, which may cause errors due to variation of land use from 1984 to 1988. Besides, spatial and temporal variations of land use also affected streamflow change (Donohue et al., 2011; Roderick and Farquhar, 2011). In the model, recharge to groundwater and change of soil water storage might be ignored for water balance at a meso-scale catchment (Sun et al., 2005). Moreover, uncertainty of the model would be exaggerated when applied to small catchments, such as BCZ catchment (65.2 km^2) and TM catchment (3.4 km^2). Although many uncertainties existed in this model, we suggest that the approximate contribution of $d\overline{Q}_{land}$ could be 64 % for 1984–1999 and 49 % for 2000–2008, respectively, which basically coincided with the result of two other models.

In the climate elasticity model (CEM), P and E_p were employed to assess climate variation. Annual P in the evaluation period I was 9 $mm\,yr^{-1}$ more than that in the reference period simultaneously with 25 $mm\,yr^{-1}$ less for annual E_p. Whereas $d\overline{Q}_{clim}$ was just −1.5 $mm\,yr^{-1}$ which indicated that P and E_p had nearly same effect for annual Q in the evaluation period I. As a quantitative assessment on hydrological impacts of climate change, without spatial input, especially for the catchment area of 15 380 km^2 with altitude range from 50 to 2292 m (Fig. 1), the climate elasticity model lacks physical mechanisms and ignores the details of the impact of climate variation (Yang et al., 2014a). Specifically, with catchment slope growing, the relative error increases with a median of 3.0 % and a maximum of 20 % when 10 % precipitations alteration in those catchments of China (Yang et al., 2014b). Extreme climate events also increase the risk of model result.

Rainfall–runoff model only takes rainfall as climate indicator into account to estimate the impact of climate change which might be the main reason differentially from other two approaches. P for 1984–1999 was 9 $mm\,yr^{-1}$ greater than that for 1961–1983 while $d\overline{Q}_{clim}$ was 2.7 $mm\,yr^{-1}$ smaller correspondingly (Table 2), which illustrated that the variance of the monthly precipitation played an important role on modeling streamflow

HESSD
12, 7785–7819, 2015

besides annual P. Moreover, it was noted that the watershed was characterized by mountainous environment with thin soil stratum (< 30 cm) (He et al., 2010). Therefore, rather than storing water in the soil, more rainfall became streamflow, offsetting water consumption due to afforestation, resulted in Q change less than expected which was another reason differentially estimating the impact of climate change on inflow into MYRC.

4.3 Implications to water resources management

Compared to the reference period, contribution of land use change to the streamflow decline for 1984–1999 was greater than that for 2000–2008. This finding indicated that land use adjustment for 2000–2008 alleviated shortage of water supply in MYRC. Meanwhile, Climate change will increase the uncertainty of the estimated land use impact (Lauri et al., 2012). That should be considered as a critical factor to optimize future water management (Gosling et al., 2011). Furthermore, anthropogenic effects, including water withdrawal and water restriction, would make both negative and positive effects on water supply to Miyun reservoir. Monitoring and objectively evaluating spatial and temporal variation of water resources are the prerequisites for water resource planning. Land use adjustment could also offset the negative effect of climate variation. For example, Paddy to Dry Land is considered as an effective mean to increase inflow into Miyun reservoir. Moreover, artificial forest plantations widely implemented during the last 30 years aggravated water stress in this semi-arid region (Wang et al., 2012). More native vegetation rather than artificial pure forest should be established to achieve the desired hydrological functioning of MYRC. In the same time, saving and rational allocation of water resource can play an important complementary role facing water crisis. In summary, comprehensive measures are necessary to deal with water shortages including vegetation restoration and water allocation.

HESSD
12, 7785–7819, 2015

5 Conclusions

The Miyun reservoir experienced a significant decreasing trend of streamflow in the past three decades. We used a comprehensive modeling approach to detect hydrological changes and their attributions. The dramatic change of land use in the 1980s and 1990s due to expansion of forestland and reduction of cropland had exacerbated streamflow decline by boosting catchment E_a. The global warming has resulted in an increase in E_p, resulting in an increase in total water loss from the student basin. We found that land use change dominated the streamflow decline in the 1980s–1990s, but climate warming contributed most to the water supply decline in the 2000s.

We conclude that climate change must be considered in designing watershed management strategies in Miyun reservoir to meet the increasing water supply demand of the megacity of Beijing. Our results suggest that land use adjustment (Converting cropland to natural grasslands) and water resources management (such as irrigation use and groundwater withdrawal) should be optimized to adapt to future climate changes to sustain the water supply functions of the MYRC.

Acknowledgements. This work is financially supported by China Postdoctoral Science Foundation (No. 2012M511938), Forestry Nonprofit Industry Research of State Forestry Administration (No. 201104109), and China Scholarship Council for Visiting Duke University. We thank Cunyong Ju for his assistance in data analysis.

References

Aguado, E., Cayan, D., Riddle, L., and Roos, M.: Climatic fluctuations and the timing of West Coast streamflow, J. Climate, 5, 1468–1483, 1992.

Arabi, M., Govindaraju, R. S., and Hantush, M. M.: A probabilistic approach for analysis of uncertainty in the evaluation of watershed management practices, J. Hydrol., 333, 459–471, 2007.

Baker, T. J. and Miller, S. N.: Using the Soil and Water Assessment Tool (SWAT) to assess land use impact on water resources in an East African watershed, J. Hydrol., 486, 100–111, 2013.

Bao, Z., Fu, G., Wang, G., Jin, J., He, R., Yan, X., and Liu, C.: Hydrological projection for the Miyun Reservoir basin with the impact of climate change and human activity, Quatern. Int., 282, 96–103, doi:10.1016/j.quaint.2012.07.012, 2012a.

Bao, Z., Zhang, J., Wang, G., Fu, G., He, R., Yan, X., Jin, J., Liu, Y., and Zhang, A.: Attribution for decreasing streamflow of the Haihe River basin, northern China: climate variability or human activities?, J. Hydrol., 460–461, 117–129, doi:10.1016/j.jhydrol.2012.06.054, 2012b.

Barnett, T. P., Adam, J. C., and Lettenmaier, D. P.: Potential impacts of a warming climate on water availability in snow-dominated regions, Nature, 438, 303–309, 2005.

Beguería, S., López-Moreno, J. I., Lorente, A., Seeger, M., and García-Ruiz, J. M.: Assessing the effect of climate oscillations and land-use changes on streamflow in the Central Spanish Pyrenees, Ambio, 32, 283–286, 2003.

Brown, A. E., Zhang, L., McMahon, T. A., Western, A. W., and Vertessy, R. A.: A review of paired catchment studies for determining changes in water yield resulting from alterations in vegetation, J. Hydrol., 310, 28–61, doi:10.1016/j.jhydrol.2004.12.010, 2005.

Chang, J., Zhang, H., Wang, Y., and Zhu, Y.: Assessing the impact of climate variability and human activity to streamflow variation, Hydrol. Earth Syst. Sci. Discuss., 12, 5251–5291, doi:10.5194/hessd-12-5251-2015, 2015.

Chaobai River Management Bureau of Beijing: Flood and Drought Hazards in the Chaobai River, China Water Resour. and Hydropow. Press, Beijing, 209, 2004.

Christensen, N. S., Wood, A. W., Voisin, N., Lettenmaier, D. P., and Palmer, R. N.: The effects of climate change on the hydrology and water resources of the Colorado River basin, Climatic Change, 62, 337–363, 2004.

Costa, M. H., Botta, A., and Cardille, J. A.: Effects of large-scale changes in land cover on the discharge of the Tocantins River, Southeastern Amazonia, J. Hydrol., 283, 206–217, doi:10.1016/s0022-1694(03)00267-1, 2003.

Dong, W. and Li, X.: Analysis of water resource of Miyun reservoir in Chaobai river basin, Environ. Sci. Technol., 29, 58–60, 2006.

Donohue, R., Roderick, M., and McVicar, T.: Can dynamic vegetation information improve the accuracy of Budyko's hydrological model?, J. Hydrol., 390, 23–34, 2010.

Donohue, R. J., Roderick, M. L., and McVicar, T. R.: Assessing the differences in sensitivities of runoff to changes in climatic conditions across a large basin, J. Hydrol., 406, 234–244, doi:10.1016/j.jhydrol.2011.07.003, 2011.

Fu, G., Charles, S. P., and Chiew, F. H. S.: A two-parameter climate elasticity of streamflow index to assess climate change effects on annual streamflow, Water Resour. Res., 43, W11419, doi:10.1029/2007WR005890, 2007.

Gao, P., Geissen, V., Ritsema, C. J., Mu, X.-M., and Wang, F.: Impact of climate change and anthropogenic activities on stream flow and sediment discharge in the Wei River basin, China, Hydrol. Earth Syst. Sci., 17, 961–972, doi:10.5194/hess-17-961-2013, 2013.

Gao, Y. and Long, D.: Intercomparison of remote sensing-based models for estimation of evapotranspiration and accuracy assessment based on SWAT, Hydrol. Process., 22, 4850–4869, doi:10.1002/hyp.7104, 2008.

Gao, Y., Yao, Z., Liu, B., and Lv, A.: Evolution trend of Miyun Reservoir inflow and its motivation factors analysis, Prog. Geog., 21, 546–553, 2002.

Gao, Y., Long, D., and Li, Z. L.: Estimation of daily actual evapotranspiration from remotely sensed data under complex terrain over the upper Chao river basin in North China, Int. J. Remote Sens., 29, 3295–3315, doi:10.1080/01431160701469073, 2008.

Gosling, S. N., Taylor, R. G., Arnell, N. W., and Todd, M. C.: A comparative analysis of projected impacts of climate change on river runoff from global and catchment-scale hydrological models, Hydrol. Earth Syst. Sci., 15, 279–294, doi:10.5194/hess-15-279-2011, 2011.

Hamon, W. R.: Computation of Direct Runoff Amounts from Storm Rainfall, International Association of Scientific Hydrology Publication, The Pennsylvania State University in 201 Old Main, University Park, PA, USA, 63, 52–62, 1963.

Haverkamp, S., Fohrer, N., and Frede, H. G.: Assessment of the effect of land use patterns on hydrologic landscape functions: a comprehensive GIS-based tool to minimize model uncertainty resulting from spatial aggregation, Hydrol. Process., 19, 715–727, doi:10.1002/hyp.5626, 2005.

He, J., Cai, Q., Li, G., and Wang, Z.: Integrated erosion control measures and environmental effects in rocky mountainous areas in northern China, Int. J. Sediment Res., 25, 294–303, doi:10.1016/s1001-6279(10)60046-7, 2010.

Jones, R. N., Chiew, F. H. S., Boughton, W. C., and Zhang, L.: Estimating the sensitivity of mean annual runoff to climate change using selected hydrological models, Adv. Water Resour., 29, 1419–1429, doi:10.1016/j.advwatres.2005.11.001, 2006.

Kavetski, D., Kuczera, G., and Franks, S. W.: Bayesian analysis of input uncertainty in hydrological modeling: 2. Application, Water Resour. Res., 42, W03408, doi:10.1029/2005WR004376, 2006.

Lauri, H., de Moel, H., Ward, P. J., Räsänen, T. A., Keskinen, M., and Kummu, M.: Future changes in Mekong River hydrology: impact of climate change and reservoir operation on discharge, Hydrol. Earth Syst. Sci., 16, 4603–4619, doi:10.5194/hess-16-4603-2012, 2012.

Li, L., Zhang, L., Wang, H., Wang, J., Yang, J., Jiang, D., Li, J., and Qin, D.: Assessing the impact of climate variability and human activities on streamflow from the Wuding River basin in China, Hydrol. Process., 21, 3485–3491, doi:10.1002/hyp.6485, 2007.

Liu, B., Yao, Z., and Gao, Y.: Trend and driving forces of water consumed structure changes in Beijing, Resource Science, 25, 38–43, 2003.

López-Moreno, J. I., Vicente-Serrano, S. M., Moran-Tejeda, E., Zabalza, J., Lorenzo-Lacruz, J., and García-Ruiz, J. M.: Impact of climate evolution and land use changes on water yield in the ebro basin, Hydrol. Earth Syst. Sci., 15, 311–322, doi:10.5194/hess-15-311-2011, 2011.

Lu, J., Sun, G., McNulty, S., and Amatya, D. M.: A Comparison of Six Potential Evapotranspiration Methods for Regional Use in the Southeastern United States, J. Am. Water Resour. As., 41, 621–633, 2005.

Ma, H., Yang, D., Tan, S. K., Gao, B., and Hu, Q.: Impact of climate variability and human activity on streamflow decrease in the Miyun Reservoir catchment, J. Hydrol., 389, 317–324, doi:10.1016/j.jhydrol.2010.06.010, 2010.

Ma, Z., Kang, S., Zhang, L., Tong, L., and Su, X.: Analysis of impacts of climate variability and human activity on streamflow for a river basin in arid region of northwest China, J. Hydrol., 352, 239–249, doi:10.1016/j.jhydrol.2007.12.022, 2008.

Mango, L. M., Melesse, A. M., McClain, M. E., Gann, D., and Setegn, S. G.: Land use and climate change impacts on the hydrology of the upper Mara River Basin, Kenya: results of a modeling study to support better resource management, Hydrol. Earth Syst. Sci., 15, 2245–2258, doi:10.5194/hess-15-2245-2011, 2011.

Mann, H. B.: Nonparametric tests against trend, Econometrica, 13, 245–259, doi:10.2307/1907187, 1945.

Mao, D. and Cherkauer, K. A.: Impacts of land-use change on hydrologic responses in the Great Lakes region, J. Hydrol., 374, 71–82, doi:10.1016/j.jhydrol.2009.06.016, 2009.

Moiwo, J. P., Lu, W., Zhao, Y., Yang, Y., and Yang, Y.: Impact of land use on distributed hydrological processes in the semi-arid wetland ecosystem of Western Jilin, Hydrol. Process., 24, 492–503, 2010.
Morán-Tejeda, E., Ceballos-Barbancho, A., and Llorente-Pinto, J. M.: Hydrological response of Mediterranean headwaters to climate oscillations and land-cover changes: the mountains of Duero River basin (Central Spain), Global Planet. Change, 72, 39–49, 2010.
Petchprayoon, P., Blanken, P. D., Ekkawatpanit, C., and Hussein, K.: Hydrological impacts of land use/land cover change in a large river basin in central–northern Thailand, Int. J. Climatol., 30, 1917–1930, 2010.
Raymond, P. A., Oh, N.-H., Turner, R. E., and Broussard, W.: Anthropogenically enhanced fluxes of water and carbon from the Mississippi River, Nature, 451, 449–452, 2008.
Risbey, J. S. and Entekhabi, D.: Observed Sacramento Basin streamflow response to precipitation and temperature changes and its relevance to climate impact studies, J. Hydrol., 184, 209–223, 1996.
Roderick, M. L. and Farquhar, G. D.: A simple framework for relating variations in runoff to variations in climatic conditions and catchment properties, Water Resour. Res., 47, W00G07, doi:10.1029/2010WR009826, 2011.
Sankarasubramanian, A., Vogel, R. M., and Limbrunner, J. F.: Climate elasticity of streamflow in the United States, Water Resour. Res., 37, 1771–1781, doi:10.1029/2000wr900330, 2001.
Schaake, J. C. and Waggoner, P.: From climate to flow, in: Climate Change and US Water Resources, John Wiley and Sons Inc., New York, USA, 177–206, 1990.
Schewe, J., Heinke, J., Gerten, D., Haddeland, I., Arnell, N. W., Clark, D. B., Dankers, R., Eisner, S., Fekete, B. M., Colon-Gonzalez, F. J., Gosling, S. N., Kim, H., Liu, X., Masaki, Y., Portmann, F. T., Satoh, Y., Stacke, T., Tang, Q., Wada, Y., Wisser, D., Albrecht, T., Frieler, K., Piontek, F., Warszawski, L., and Kabat, P.: Multimodel assessment of water scarcity under climate change, P. Natl. Acad. Sci. USA, 111, 3245–3250, doi:10.1073/pnas.1222460110, 2014.
Searcy, J. K. and Hardison, C. H.: Double-mass curves Manual of Hydrology: Part 1. General surface-water Techniques, Geological survey water-supply paper, 1541-B, 31–64, Washington D.C., 1960.
Shen, Z. Y., Chen, L., and Chen, T.: Analysis of parameter uncertainty in hydrological and sediment modeling using GLUE method: a case study of SWAT model applied to Three

HESSD
12, 7785–7819, 2015

Gorges Reservoir Region, China, Hydrol. Earth Syst. Sci., 16, 121–132, doi:10.5194/hess-16-121-2012, 2012.
Sneyers, R.: Sur l'analyse statistique des séries d'observations, Secrétariat de l'Organisation Météorologique Mondiale, Gencve, Suisse, 1975.
Stohlgren, T. J., Chase, T. N., Pielke, R. A., Kittel, T. G., and Baron, J.: Evidence that local land use practices influence regional climate, vegetation, and stream flow patterns in adjacent natural areas, Glob. Change Biol., 4, 495–504, 1998.
Sun, G., McNulty, S. G., Lu, J., Amatya, D. M., Liang, Y., and Kolka, R. K.: Regional annual water yield from forest lands and its response to potential deforestation across the southeastern United States, J. Hydrol., 308, 258–268, doi:10.1016/j.jhydrol.2004.11.021, 2005.
Sun, G., Zhou, G., Zhang, Z., Wei, X., McNulty, S. G., and Vose, J. M. Potential water yield reduction due to forestation across China, J. Hydrol., 328, 548–558, doi:10.1016/j.jhydrol.2005.12.013, 2006.
Sun, S., Chen, H., Ju, W., Song, J., Zhang, H., Sun, J., and Fang, Y.: Effects of climate change on annual streamflow using climate elasticity in Poyang Lake Basin, China, Theor. Appl. Climatol., 112, 169–183, 2013.
Tang, L., Yang, D., Hu, H., and Gao, B.: Detecting the effect of land-use change on streamflow, sediment and nutrient losses by distributed hydrological simulation, J. Hydrol., 409, 172–182, doi:10.1016/j.jhydrol.2011.08.015, 2011.
Velázquez, J. A., Schmid, J., Ricard, S., Muerth, M. J., Gauvin St-Denis, B., Minville, M., Chaumont, D., Caya, D., Ludwig, R., and Turcotte, R.: An ensemble approach to assess hydrological models' contribution to uncertainties in the analysis of climate change impact on water resources, Hydrol. Earth Syst. Sci., 17, 565–578, doi:10.5194/hess-17-565-2013, 2013.
Verburg, P. H., Neumann, K., and Nol, L.: Challenges in using land use and land cover data for global change studies, Glob. Change Biol., 17, 974–989, doi:10.1111/j.1365-2486.2010.02307.x, 2011.
Wang, G., Xia, J., and Chen, J.: Quantification of effects of climate variations and human activities on runoff by a monthly water balance model: a case study of the Chaobai River basin in northern China, Water Resour. Res., 45, W00A11, doi:10.1029/2007wr006768, 2009.

HESSD
12, 7785–7819, 2015

Wang, S., Zhang, Z., McVicar, T. R., Zhang, J., Zhu, J., and Guo, J.: An event-based approach to understanding the hydrological impacts of different land uses in semi-arid catchments, J. Hydrol., 416–417, 50–59, doi:10.1016/j.jhydrol.2011.11.035, 2012.

Wang, S., Zhang, Z., R. McVicar, T., Guo, J., Tang, Y., and Yao, A.: Isolating the impacts of climate change and land use change on decadal streamflow variation: assessing three complementary approaches, J. Hydrol., 507, 63–74, doi:10.1016/j.jhydrol.2013.10.018, 2013.

Wang, Y.: A spatiotemporal analysis of land use change and zoning of landscape restoration and protection in Miyun Reservoir watershed, PhD thesis, Chinese Academy of Forestry, Beijing, China, 2010.

Wei, X., Liu, W., and Zhou, P.: Quantifying the relative contributions of forest change and climatic variability to hydrology in large watersheds: a critical review of research methods, Water, 5, 728–746, doi:10.3390/w5020728, 2013.

Wigbout, M.: Limitation in the use of double-mass curves, J. Hydrol., 12, 132–138, 1973.

Xu, Z. X., Pang, J. P., Liu, C. M., and Li, J. Y.: Assessment of runoff and sediment yield in the Miyun Reservoir catchment by using SWAT model, Hydrol. Process., 23, 3619–3630, doi:10.1002/hyp.7475, 2009.

Yang, H., Yang, D., and Hu, Q.: An error analysis of the Budyko hypothesis for assessing the contribution of climate change to runoff, Water Resour. Res., 50, 9620–9629, doi:10.1002/2014wr015451, 2014a.

Yang, H., Qi, J., Xu, X., Yang, D., and Lv, H.: The regional variation in climate elasticity and climate contribution to runoff across China, J. Hydrol., 517, 607–616, doi:10.1016/j.jhydrol.2014.05.062, 2014b.

Yang, Y. and Tian, F. Abrupt change of runoff and its major driving factors in Haihe River Catchment, China, J. Hydrol., 374, 373–383, doi:10.1016/j.jhydrol.2009.06.040, 2009.

Zégre, N., Skaugset, A. E., Som, N. A., McDonnell, J. J., and Ganio, L. M.: In lieu of the paired catchment approach: hydrologic model change detection at the catchment scale, Water Resour. Res., 46, W11544, doi:10.1029/2009wr008601, 2010.

Zhan, C., Xu, Z., Ye, A., and Su, H.: LUCC and its impact on run-off yield in the Bai River catchment–upstream of the Miyun Reservoir basin, J. Plant Ecol.-UK, 4, 61–66, doi:10.1093/jpe/rtr003, 2011.

Zhang, J. and Wang, G.: Impacts of Climate Changes on Hydrology and Water Resources, Science Press, Beijing, 188–189, 2007.

Zhang, L., Dawes, W. R., and Walker, G. R.: Response of mean annual evapotranspiration to vegetation changes at catchment scale, Water Resour. Res., 37, 701–708, doi:10.1029/2000wr900325, 2001.

Zhang, X., Zhang, L., Zhao, J., Rustomji, P., and Hairsine, P.: Responses of streamflow to changes in climate and land use/cover in the Loess Plateau, China, Water Resour. Res., 44, W00A07, doi:10.1029/2007wr006711, 2008.

Zheng, J., Yu, X., Jia, G., and Xia, B.: Dynamic evolution of ecological service value based on LUCC in Miyun Reservoir Catchment, Transactions of the CSAE, 26, 315–320, 2010.

Zheng, J., Yu, X., Deng, W., Wang, H., and Wang, Y.: Sensitivity of land-use change to streamflow in Chaobai river basin, J. Hydrol. Eng., 18, 457–464, doi:10.1061/(asce)he.1943-5584.0000669, 2013.

HESSD

12, 7785–7819, 2015

Table 1. Estimations on the contribution of land use change and climate variability to streamflow decreasing. The numbers directly following the ± signs are the standard deviation. The numbers in bracket represent the contribution percentage.

Period	$\overline{P}$	$\overline{E_p}$	$\overline{Q}$	$d\overline{Q}_{tot}$	Annual water balance model		The climate elasticity model		Rainfall–runoff model	
					$d\overline{Q}_{land}$	$d\overline{Q}_{clim}$	$d\overline{Q}_{land}$	$d\overline{Q}_{clim}$	$d\overline{Q}_{land}$	$d\overline{Q}_{clim}$
Reference (1961–1983)	446±75	847±23	59.1±30.3	–	–	–	–	–	–	–
Evaluation I (1984–1999)	455±84	872±24	41.0±21.0	−18.1	−11.5 (64 %)	−6.6 (36 %)	−16.6 (92 %)	−1.5 (8 %)	−15.4 (85 %)	−2.7 (15 %)
Evaluation II (2000–2008)	412±41	890±17	19.4 ± 8.8	−39.7	−19.6 (49 %)	−20.1 (51 %)	−23.2 (58 %)	−16.5 (42 %)	−14.4 (36 %)	−25.3 (64 %)

HESSD
12, 7785–7819, 2015

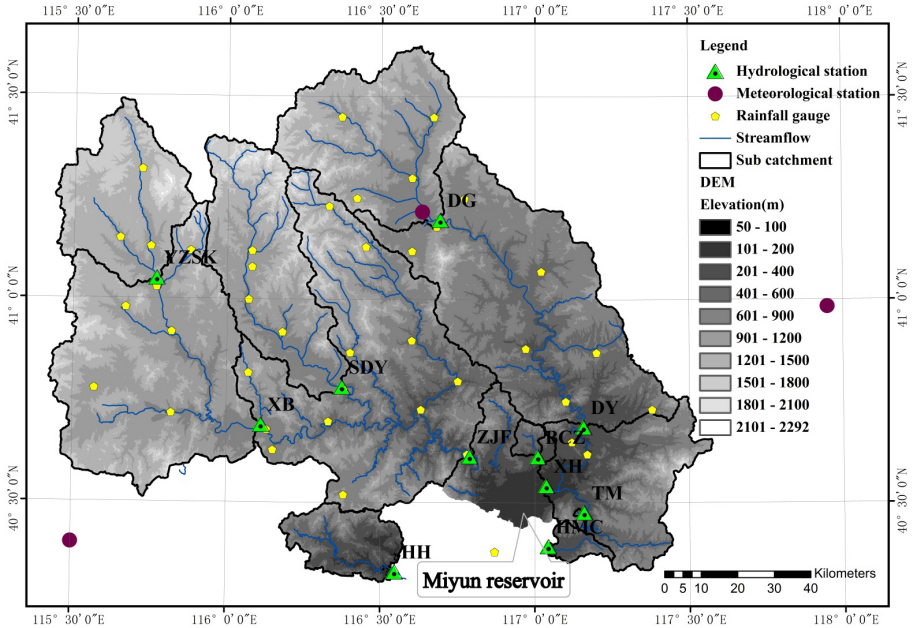

Figure 1. Information of Miyun reservoir catchment and sub catchments including YZSK (Yunzhoushuiku, 1193 km^2), XB (Xiabao, 3960 km^2), SDY (Sandaoying, 1536 km^2), ZJF (Zhangjiafen, 8762 km^2), DG (Dage, 1660 km^2), DY (Daiying, 4634 km^2), XH (Xiahui, 5891 km^2), HH (Huaihe, 486 km^2), HMC (Hongmenchuan, 111 km^2), BCZ (Banchengzi, 65 km^2), and TM (Tumen, 3 km^2).

HESSD
12, 7785–7819, 2015

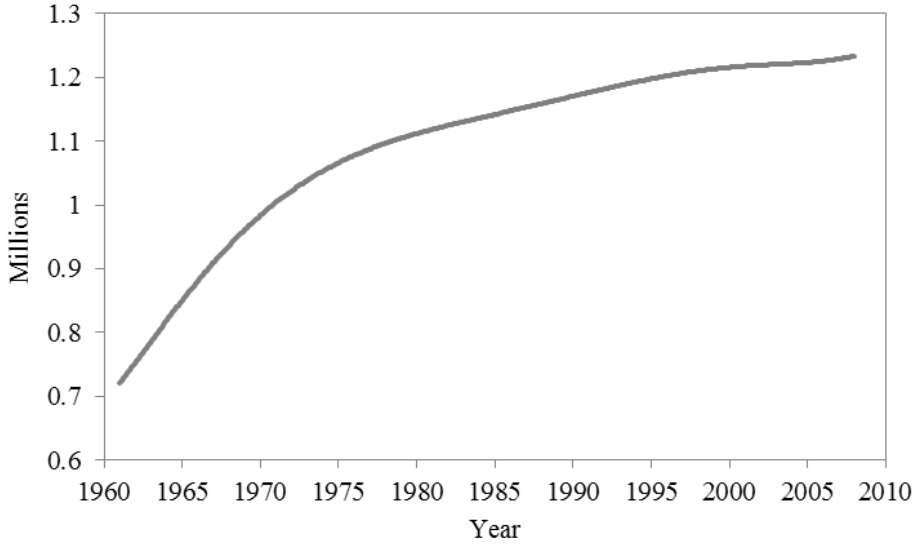

Figure 2. Change in the population of 4 main counties located in Hebei province from 1961 to 2007.

HESSD
12, 7785–7819, 2015

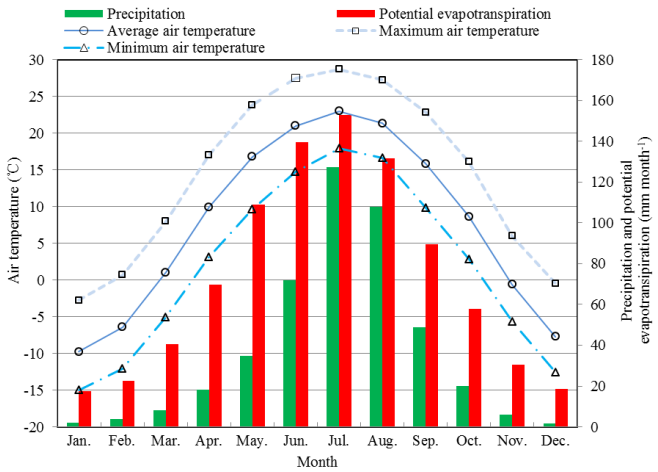

month	Average air temperature	Maximum air temperature	Minimum air temperature	Precipitation	Potential evapotranspiration
Jan.	-9.7457757	-2.7769927	-14.94844683	1.862698	17.52
Feb.	-6.3912728	0.7101924	-12.11661221	3.77381	22.64
Mar.	1.01906469	7.99848097	-5.060808158	8.131746	40.4
Apr.	9.94022046	17.0288183	3.117433862	18.28915	69.6
May.	16.7950802	23.8500384	9.607671958	34.91825	109.04
Jun.	20.9692504	27.4908907	14.69842152	71.75503	139.48
Jul.	22.9753089	28.6749189	17.9087899	127.1421	152.72
Aug.	21.3538752	27.2623059	16.58661888	107.727	131.6
Sep.	15.8313051	22.8249206	9.864100529	48.83519	89.44
Oct.	8.65164533	16.0926182	2.77177846	19.91111	57.84
Nov.	-0.608933	5.97111993	-5.682257496	5.985979	30.56
Dec.	-7.6903823	-0.4657194	-12.59953234	1.772222	18.56

Figure 3. Monthly average precipitation, potential evapotranspiration and air temperature during 1961–2008 in Miyun reservoir catchment.

HESSD
12, 7785–7819, 2015

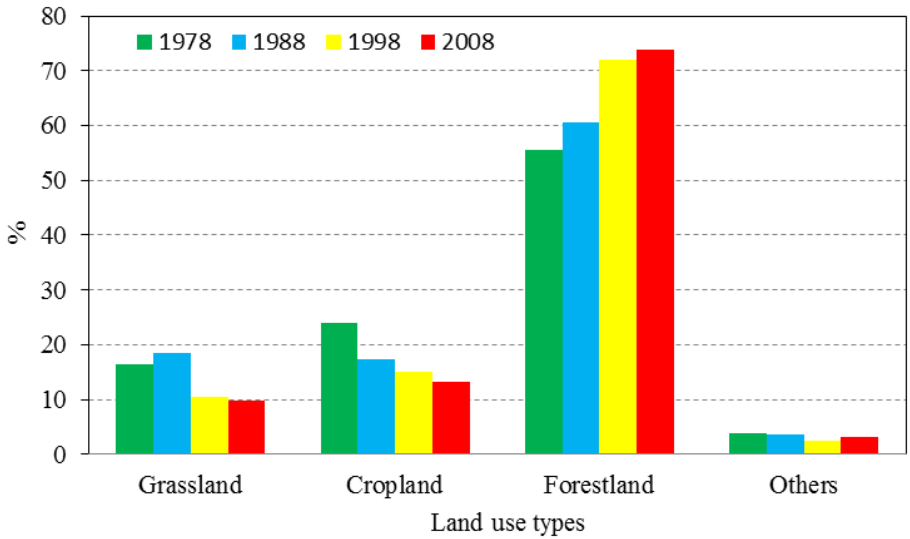

Land use types	1978	1988	1998	2008
grassland	16.54096	18.48505	10.37711	9.830949
cropland	23.94668	17.28869	15.16255	13.13394
forestland	55.61118	60.59168	71.93108	73.79064
others	3.90117	3.63459	2.529259	3.244473

Figure 4. Land use composition of Miyun reservoir catchment (15 380 km^2) in 1978, 1988, 1998, and 2008.

HESSD
12, 7785–7819, 2015

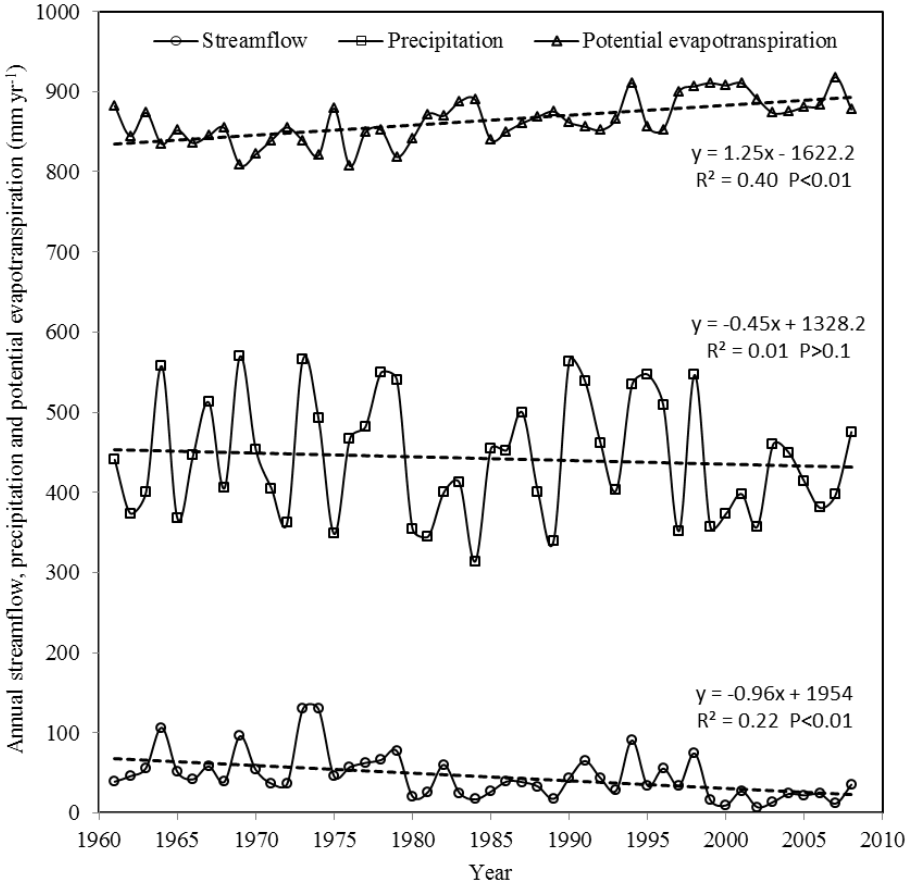

Figure 5. Evolution of streamflow (Q), precipitation (P), and potential evapotranspiration (E_p) of Miyun reservoir catchment over 1961–2008. The dashed lines are the fitted trend for variable.

HESSD
12, 7785–7819, 2015

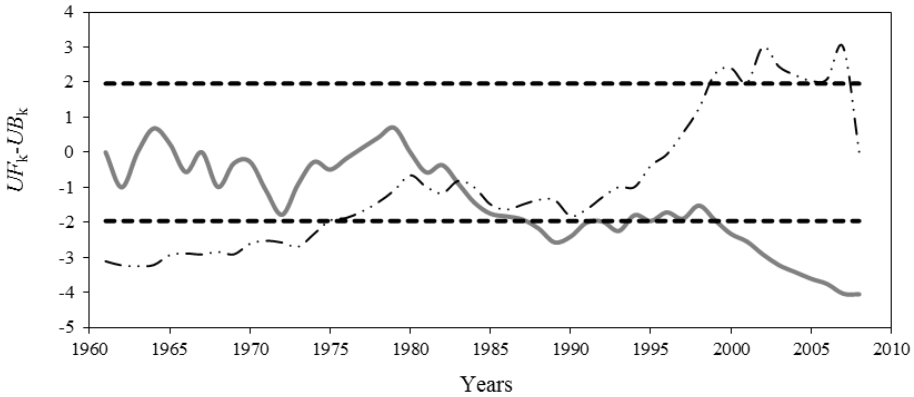

Figure 6. The Sequential Mann–Kendall test for annual streamflow in Miyun reservoir catchment with forward-trend UK_k (solid line), and backward-trend UB_k (dashed line). Dotted horizontal lines represent critical values at the 95 % confidence.

HESSD
12, 7785–7819, 2015

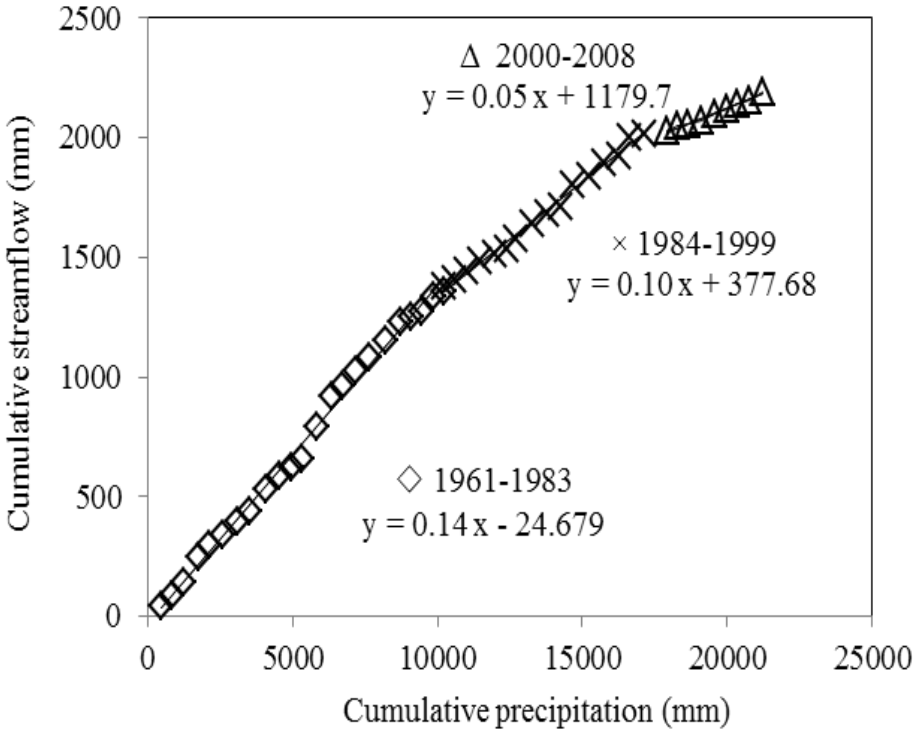

Figure 7. The Double Mass Curve showing the relations between cumulative streamflow and cumulative precipitation for Miyun reservoir catchment (1961–2008).

HESSD
12, 7785–7819, 2015

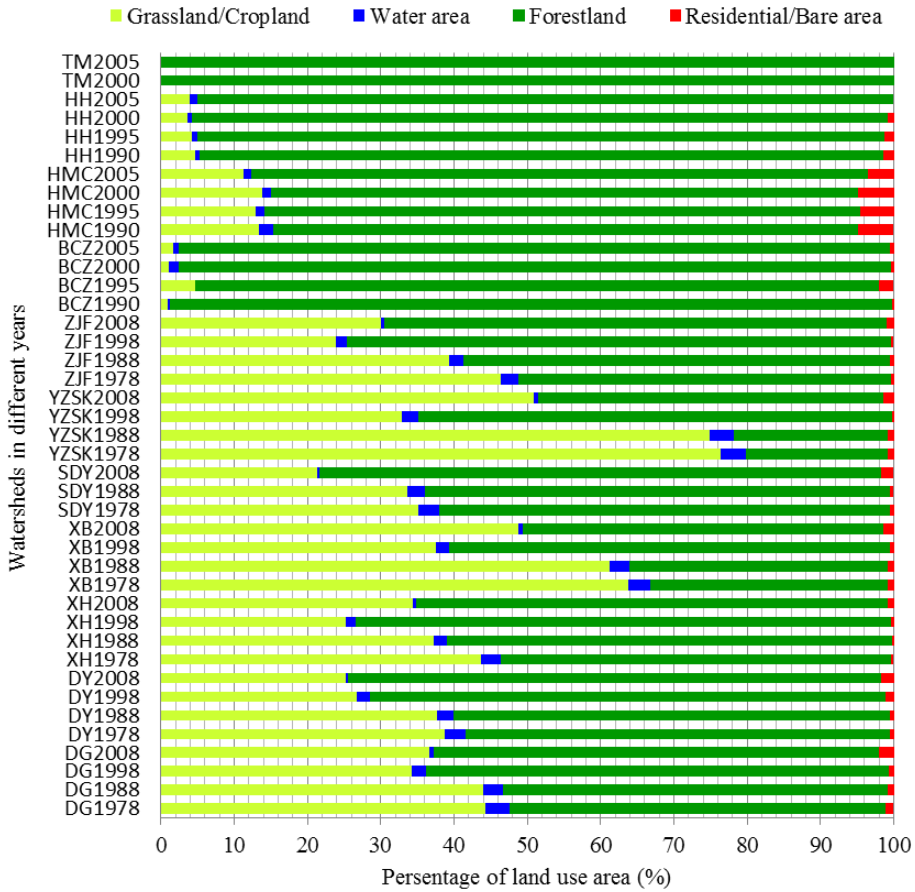

Figure 8. Land use composition of watersheds in different year used for annual water balance model building. For example, DG1978 refer to Dage Watershed in 1978. Data prior to 2001 was used for the model calibration. Data after 2001 was used for the model validation.

HESSD
12, 7785–7819, 2015

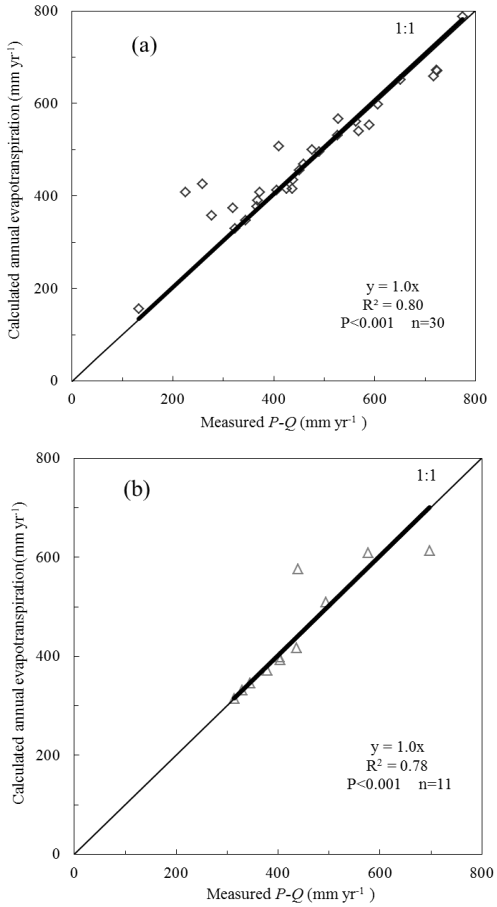

Figure 9. Scatter plots of calculated evapotranspiration using Eqs. (7) and (8) against measured evapotranspiration $E_a = P - Q$ during calibration phase **(a)** and validation phase **(b)**. The dashed line is the 1 : 1 line and the solid line is the line of best-fit provided by the equation.

HESSD
12, 7785–7819, 2015